IEEE Access
Multidisciplinary | Rapid Review | Open Access Journal

Received May 1, 2019, accepted May 14, 2019, date of publication May 17, 2019, date of current version May 30, 2019.

Digital Object Identifier 10.1109/ACCESS.2019.2917505

A Compensated Multi-Anchors TOF-Based Localization Algorithm for Asynchronous Wireless Sensor Networks

TAN WANG, HONG DING, HUI XIONG, AND LINHUA ZHENG
College of Electronic Science, National University of Defense Technology, Changsha 410073, China

Corresponding author: Tan Wang (wangtan3@163.com)

This work was supported by the National Natural Science Foundation of China under Grant 61571452.

ABSTRACT Tag localization for asynchronous wireless sensor networks requires the development of a scheme for clock synchronization. This remains a difficult and open problem since the performance of tag localization can be adversely affected by complications such as reply time and relative clock skew. Joint clock synchronization and a tag localization algorithm that implements a multi-anchor compensated time-of-flight (TOF) to the asynchronous wireless sensor network is a possible and viable solution. Although previous methods that leverage TOF measurements are effective and easily conducted, their performance is not always superior due to the relative clock skew. In this paper, we propose to extend the joint clock/tag synchronization/localization algorithm by introducing a compensation factor that can cancel relative clock skews from multi-tag anchor pairs. We apply a least squares estimation (LSE) algorithm to both the time of emission (TOE) and time of arrival (TOA) for the clock synchronization step. Under the assumption of a Gaussian measurement noise model, the tag localization problem is approximately solved by maximum likelihood estimation (MLE). To assess the performance of our algorithm, we derive the mean square error (MSE) of both relative clock skew and tag location and numerically evaluate the Cramér–Rao lower bound (CRLB) as a benchmark. The simulation results show that the accuracy of the relative clock skew-based estimation and tag localization are significantly improved over traditional algorithms when the appropriate reply time is selected. This is what our proposed algorithm focuses on: it is robust to tag mobility to some extent. We test the performance of proposed algorithm using a well-designed experiment. Based on the experiment results, the localization algorithm can achieve high accuracy without an additional restriction on the reply time and the clock skew.

INDEX TERMS Source localization, wireless sensor network (WSN), time-of-flight (TOF), symmetric double-sided two-way ranging (SDS-TWR), relative clock skew.

I. INTRODUCTION

With the advances in wireless communications and micro-system technologies, wireless sensor networks (WSNs) have developed rapidly in recent decades [1], [2]. One potential application of WSNs is source localization, which plays an important role in signal processing and wireless communication. Many well-known applications that use WSNs include emergency service [3], [4], environmental monitoring, target tracking [5]. A popular technology for source localization is global positioning systems (GPS). Although we can achieve accurate localization by equipping all sensors in the network with a GPS receiver, it is too expensive and unpractical. Additionally, its performance may degrade in indoor environments [6]. Therefore, many effective technologies are proposed to obtain accurate location estimation of WSN sensor nodes [7]. They are perhaps divided into two categories: range-based localization and range-free localization algorithms. In general, the range-based algorithms are more favorable than the range-free algorithms [8]–[11]. For range-based algorithms, there are mainly four metrics: the received signal strength (RSS) [12], [13], direction of arrival (DOA) [14], time of arrival (TOA), time of flight (TOF) [15], and time difference of arrival (TDOA) [8], [16]. Given the measured

The associate editor coordinating the review of this manuscript and approving it for publication was Giancarlo Fortino.

metrics of WSNs, location estimation approaches are typically implemented. There are several kinds of position estimation algorithms and good summaries can be found in [17], [18]. RSS methods can easily be implemented with an energy detector, but it is difficult to achieve desires localization precision. It is necessary for DOA methods to equip antenna arrays for sensor nodes, which limits the scale to large WSNs. TOA and TDOA methods, which are known as the more popular methods, estimate the position of a tag based on triangulation when at least three node positions are known.

Clock synchronization is the most challenging issue for TOF and TDOA source localization algorithms used in asynchronous wireless sensor networks; this is because many of these algorithms are time-based. Although external sophisticated clock sources, like high-quality crystals and atom clocks, can be used to improve the localization accuracy, these are expensive and unconventional solutions. Many approaches have been proposed to deal with the clock synchronization problem, e.g., timing-sync protocol for sensor networks (TPSN) [19], optimal performance reference broadcast synchronization (OPRBS) [20], and flooding time synchronization protocol [21]. In [22], a robust localization algorithm based on TDOA is proposed; the clock parameters are estimated by broadcasting signals to all the anchors periodically. However, this least-square estimation method is not effective and need more information. Zhang *et al.* [23] proposed a method to jointly estimate source location and clock offset by applying a second-order cone relaxation technique, but the influence of clock skew is not considered. Gholami *et al.* [24] proposed a two-way ranging scheme (TWR) and it can be used for tag localization. Although the TWR method eliminates the impact of clock offset, the localization precision is still limited by the reply time and the clock skew. To reduce the localization error introduced by the reply time, Hach *et al.* [25] proposed a symmetric double-sided two-way ranging (SDS-TWR) method. However, the SDS-TWR method require two same reply time for different devices and the clock skew is not considered too.

Based on the above mentioned referred literatures, mitigating the relative clock skews in time-based localization algorithm for asynchronous wireless sensor networks can provide a way to further improve the localization accuracy. Some existed studies in regard to the clock skew estimating have proposed. A novel clock skew estimation method based on carrier frequency estimation is proposed in [26]. It focuses on clock skew estimation and crystal tolerance stability, but assumes that the ranging counter is operated from the same oscillator. The Skew-Aware TWR method [27] provides a way to estimate clock skew using a linear regression approach, which can mitigate the ranging estimation error. However, the accuracy of the Skew-Aware TWR method has no significant improvement over the SDS-TWR method. Gao *et al.* [28] proposed a robust least squares (RLS) method that uses clock skews as a nuisance parameter. In the method, the clock skews of the RLS problem can also be solved using a second-order cone relaxation technique. However, the complexity of Gao's method is high. Given the previously discussed existing techniques and their potential shortcomings, an efficient TOF-based localization algorithm is proposed.

In this paper, we propose a novel TOF localization algorithm for asynchronous wireless sensor networks that compensates for multiple tag-anchor pairs. In WSNs, anchors are used as reference sensors to synchronize clocks and localize tags. Therefore, anchors must be fixed to a known position. Tags have many inherent features, such as mobility, size, natural abolition and low cost. So tags must be energy efficient and small in size with low-cost quartz oscillators. To implement the proposed algorithm, tags send signals to anchors and receive the reply messages within a short period. Then, tags send the signals to anchors once again, which resembles the SDS-TWR method. A localization server, where the clock skews estimation and tags localization determining procedures are implemented. It collects six timestamps traveling by traveling around each tag-anchor pair. The error in the original TOF measurements, due to the relative clock skew between tag and anchor, can be effectively mitigated via a compensated operation. Under the assumption of the Gaussian measurement noise model, maximum likelihood estimation (MLE) is employed for tag localization.

In this paper, we need make some assumptions about WSN TOF-based localization obstacles.

1) Since low-cost crystal oscillators are used for sensor node timing, the typical clock skew is within 10ppm.
2) The maximum radio radius is approximately 300 meters from sensor node. This is a common value for short range communication in the ISM band, i.e., IEEE 802.11b/n/g and IEEE802.15.4a.
3) The server used for localization has enough computing capability to run a complete localization algorithm and complete error compensation by using the timestamps from anchors and tags.
4) The anchor's energy consumption does not need to be considered since the anchor has more than sufficient power and the timestamp delivery is fast and effective.
5) The clock skew of a sensor node does not significantly change over time; therefore, clock skew is assumed to be constant during the localization period.
6) The position of tag is fixed during one localization period because of the weak mobility (However, the tag position may be changed in the next localization period).

The remainder of this paper is structured as follows. The ranging schemes based on the TOF and WSN localization models are given in section II. Section III describes the error compensation method implemented in the ranging and localization algorithm. Section IV shows simulation results of the relative clock skew estimation and tag localization processes. The statistical performance analysis of the proposed algorithm is also presented in this section. Section V discusses the experiment implementation and results. Section VI concludes this paper.

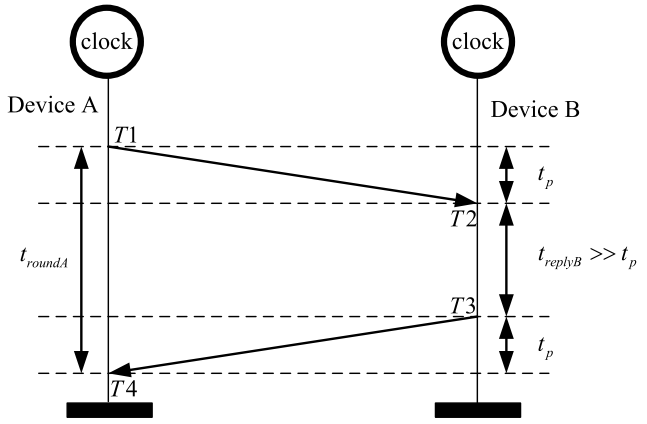

FIGURE 1. A workflow of TWR method.

Notations: Throughout this paper, the following notations will be used. The special matrices $\mathbf{1}_N$, $\mathbf{I}_N$, denote the $N \times 1$ vector of ones, $N \times N$ identity matrix. The operators $\otimes$ denotes the Kronecker product. The Euclidean norm of a vector is denoted by $||\bullet||$, the operator cov($\bullet$) is the covariance of a vector. $[\bullet]_{mn}$ denotes the *mth* row, *nth* column element of matrix. Tr($\bullet$) denotes the trace of matrix (sum of diagonal elements), E($\bullet$) denotes the expectance of matrix. a, $\tilde{a}$, $\bar{a}$, $\hat{a}$ denotes measurement value, noise-free or true value, ideal value, estimate value of a, respectively.

II. RANGING SCHEMES BASED ON TOF AND SENSOR NETWORK MODEL FOR LOCALIZATION

A. TWR AND SDS-TWR RANGING SCHEME

In this paper, the affine clock model [29] is applied. The local clock time of wireless node i can be presented as:

$$F_i(t) = (1 + e_i)t + \zeta_i \tag{1}$$

where ζ_i is initial clock offset, e_i is the oscillator frequency offset, $(1 + e_i)$ is often referred to as clock skew, and t is the ideal standard time.

According to IEEE 802.15.4a, TWR (two-way ranging) is one of the most basic ranging schemes. It is often used to mitigate asynchronous clock phenomenon. In this method, two separate objects measure the TOE/TOAs using their own local clock. As explained in previous literatures, the processing of the TWR method is straightforward [30]. As shown in Fig. 1, the estimate value of the time-of-flight (TOF) $\hat{t}_p$ can be represented by measurement timestamps (TOE/TOAs) $T1 \sim T4$:

$$\hat{t}_p = \frac{1}{2}[(T4 - T1) - (T3 - T2)] \tag{2}$$

The ideal value of t_p can be expressed as:

$$\bar{t}_p = \frac{1}{2}[(\bar{T}4 - \bar{T}1) - (\bar{T}3 - \bar{T}2)] \tag{3}$$

where $\bar{T}1 \sim \bar{T}4$ denote the ideal value of timestamps according to the universal standard clock source.

Considering the measurement noise and influence of clock skew, (2) becomes:

$$\begin{aligned}\hat{t}_p &= \frac{1}{2}[(\tilde{T}4 - \tilde{T}1) - (\tilde{T}3 - \tilde{T}2)] + \frac{1}{2}(n_4 - n_1 - n_3 + n_2) \\ &= \frac{1}{2}[(\bar{T}4 - \bar{T}1)(1 + e_A) - (\bar{T}3 - \bar{T}2)(1 + e_B)] \\ &\quad + \frac{1}{2}(n_4 - n_1 - n_3 + n_2)\end{aligned} \tag{4}$$

where $(1 + e_A)$ and $(1 + e_B)$ represent the clock skews of the device A and B, $\tilde{T}1 \sim \tilde{T}4$ denote the noise-free or true value of timestamps. $n1 \sim n4$ denote the measurement noise that can be modeled as additive white Gaussian noise (AWGN) with a zero mean and variance of σ^2. Combining (3) and (4), the estimation error of t_p is:

$$\begin{aligned}\xi_{TWR} &= \hat{t}_p - \bar{t}_p \\ &= \frac{1}{2}[(\bar{T}3 - \bar{T}2)e_{AB} + (\bar{T}4 - \bar{T}1 - \bar{T}3 + \bar{T}2)e_A] \\ &\quad + \frac{1}{2}(n_4 - n_1 - n_3 + n_2) \\ &= \frac{1}{2}(\bar{T}3 - \bar{T}2)e_{AB} + \bar{t}_p e_A + \frac{1}{2}(n_4 - n_1 - n_3 + n_2)\end{aligned} \tag{5}$$

where $e_{AB} = e_A - e_B$ represents the relative clock skew between device A and B. It is assumed that the coverage range of sensor node is within 300m, we have $\bar{t}_p < 1\mu s$. Since the clock skew of typical quartz oscillator is smaller than 10ppm, so $|\bar{t}_p e_A| < 10^{-11}$ can be ignored (the range error caused by the ignorance is within 3mm). We have

$$\xi_{TWR} = \hat{t}_p - \bar{t}_p \approx \frac{1}{2}(\bar{T}3 - \bar{T}2)e_{AB} + \frac{1}{2}(n_4 - n_1 - n_3 + n_2) \tag{6}$$

Furthermore, Hach *et al.* [25] proposed a Symmetric double-sided two-way ranging (SDS-TWR) method to reduce the ξ_{TWR}. The details of the SDS-TWR scheme is shown in Fig. 2. We can extract ideal value of $\bar{t}_p$ using ideal timestamps (TOE/TOAs).

$$2\bar{t}_p = \bar{T}4 - \bar{T}1 - \bar{T}3 + \bar{T}2 \tag{7}$$

$$2\bar{t}_p = \bar{T}6 - \bar{T}3 - \bar{T}5 + \bar{T}4 \tag{8}$$

Combining (7) and (8), we have

$$4\bar{t}_p = \bar{T}6 - \bar{T}5 + 2\bar{T}4 - 2\bar{T}3 + \bar{T}2 - \bar{T}1 \tag{9}$$

When introducing the clock skew and the measurement noise, the estimated value $\hat{t}_p$ follows by:

$$\begin{aligned}4\hat{t}_p &= T6 - T5 + 2T4 - 2T3 + T2 - T1 \\ &= \tilde{T}6 - \tilde{T}5 + 2\tilde{T}4 - 2\tilde{T}3 + \tilde{T}2 - \tilde{T}1 \\ &\quad + (n6 - n5 + 2n4 - 2n3 + n2 - n1) \\ &= (2\bar{T}4 - \bar{T}1 - \bar{T}5)(1 + e_A) + (\bar{T}6 - 2\bar{T}3 + \bar{T}2)(1 + e_B) \\ &\quad + (n6 - n5 + 2n4 - 2n3 + n2 - n1)\end{aligned} \tag{10}$$

Without loss of generality, we define

$$(\bar{T}3 - \bar{T}2) - (\bar{T}5 - \bar{T}4) = \Delta T_r \tag{11}$$

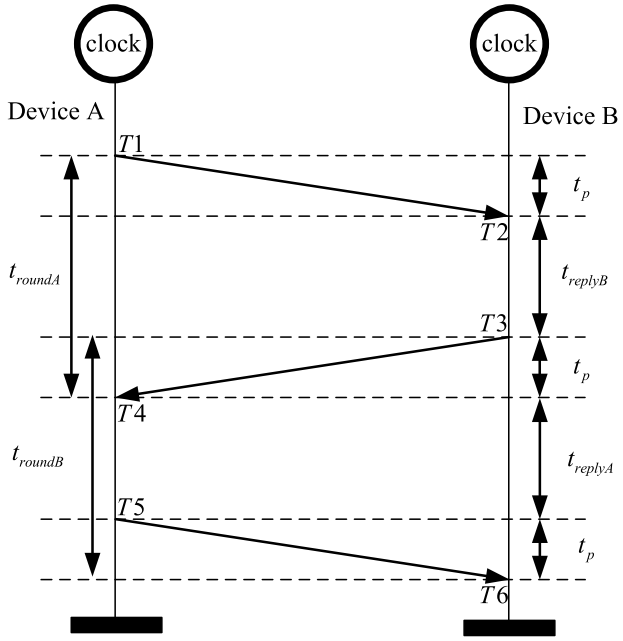

FIGURE 2. A workflow of SDS-TWR method.

TABLE 1. Estimation errors versus frequency tolerance of two methods.

Method	Reply time	e_{AB}	Error
TWR	$T_r = 100\mu s$	20ppm	1ns
	$T_r = 100\mu s$	40ppm	2ns
	$T_r = 100\mu s$	80ppm	4ns
	$T_r = 5ms$	20ppm	50ns
	$T_r = 5ms$	40ppm	100ns
	$T_r = 5ms$	80ppm	200ns
SDS-TWR	$\Delta T_r = 1\mu s$	20ppm	0.005ns
	$\Delta T_r = 1\mu s$	40ppm	0.01ns
	$\Delta T_r = 1\mu s$	80ppm	0.02ns
	$\Delta T_r = 10\mu s$	20ppm	0.05ns
	$\Delta T_r = 10\mu s$	40ppm	0.1ns
	$\Delta T_r = 10\mu s$	80ppm	0.2ns

Combining (9) and (10), the estimation error of t_p is

$$\xi_{SDS} = \hat{t}_p - \bar{t}_p = \frac{1}{2}\bar{t}_p(e_A + e_B) + \frac{1}{4}\Delta T_r e_{AB} + \frac{1}{4}(n6 - n5 + 2n4 - 2n3 + n2 - n1) \quad (12)$$

where $e_{AB} = e_A - e_B$, ξ_{SDS} denotes the estimation error of $\bar{t}_p$ using the SDS-TWR method. Since $\bar{t}_p < 1\mu s$ is assumed, $|\bar{t}_p(e_A + e_b)| < 2 \times 10^{-11}$ can be ignored. So we have:

$$\xi_{SDS} = \hat{t}_p - \bar{t}_p \approx \frac{1}{4}\Delta T_r e_{AB} + \frac{1}{4}(n6 - n5 + 2n4 - 2n3 + n2 - n1) \quad (13)$$

To achieve better performance when implementing the SDS-TWR scheme, the two reply times $(\bar{T}3 - \bar{T}2) = t_{replyB}$ and $(\bar{T}5 - \bar{T}4) = t_{replyA}$ should be set as close to each other as possible. The typical estimation errors versus frequency tolerance of the two schemes are shown in Table 1.

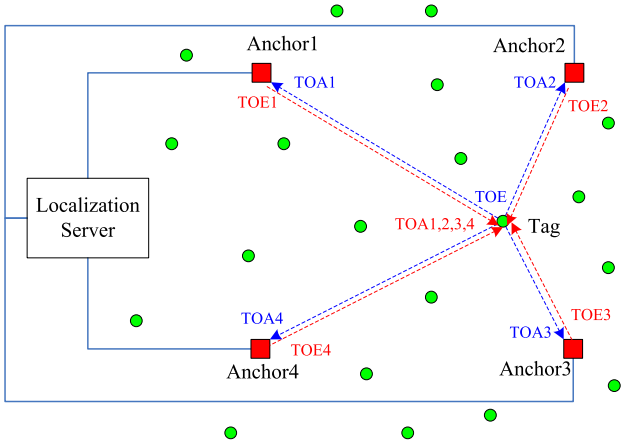

FIGURE 3. Radio wireless sensor network model for tag localization (red square nodes represent anchor and green circle nodes represent tags).

There is a direct tie between the ranging precision and the TOF estimation error. A more precise range can determine a more accurate tag location. In fact, the ranging precision is smaller than 1 m if the estimated t_p lies within 3ns of the true time of flight. A high performance crystal oscillator provides a small and stable crystal tolerance, but this kind of crystal oscillator is usually too expensive to equip in all the WSN anchors and tags. According to the estimation errors analysis for the TWR and SDS-TWR methods, the t_{reply} term can eliminate the error effectively. However, another important factor, the crystal tolerance, has received less attention in previous works. To achieve an accurate ranging precision with a TOF-based method, finding devices with low-cost crystal tolerance should be taken into consideration.

In this paper, we propose an extended-TOF localization method for asynchronous wireless sensor networks. WSNs have two kinds of sensor nodes: anchor node and tag node.

Anchors and tags measure the TOE and TOA on their own clocks respectively. Anchors that are always connected to the network infrastructure results have more than sufficient power. Thus, we treat the anchors as reference points to locate tag nodes. To reduce network overhead and cost, the number of anchors are limited. The positions of anchor are known and set carefully to ensure a more valuable service area. Tags are mobile sensor nodes and their positions are unknown and need to be located. There are many limitations for tags in practical implementations, e.g., size, cost, and energy consumption. Tags need to be designed with low-cost, low-consumption, and long-lifetime characteristics.

B. SENSOR NETWORK MODEL FOR LOCALIZATION

The WSN model used in this paper is shown in Fig. 3. For clarity, the communication procedures between the tag and anchors are listed using a series of steps shown in Fig. 4.

Step 1: As shown in Fig. 4(a), the tag broadcasts the POLL1 message and measures the TOE ($T1_0$). All anchors receive broadcasting the signal and measure the TOA ($T2_{0,1}, T2_{0,2}, T2_{0,3}, T2_{0,4}$) via their own clocks.

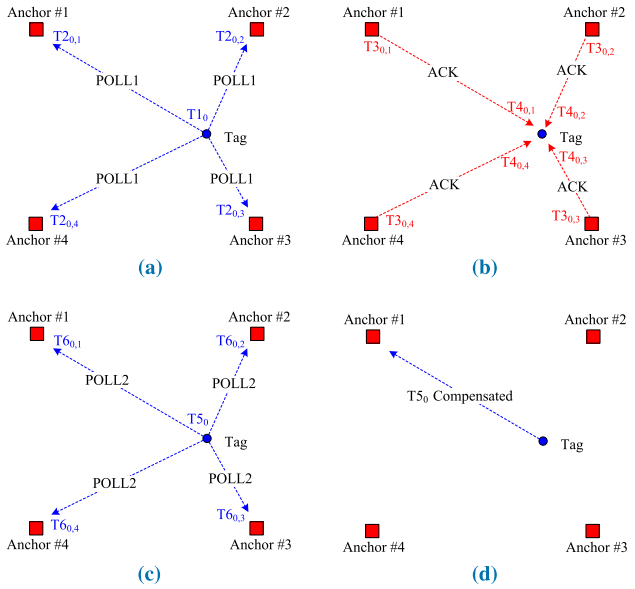

FIGURE 4. Separate steps of WSN signal transmissions. (a) Step 1, (b) Step 2, (c) Step3, and (d) Step4.

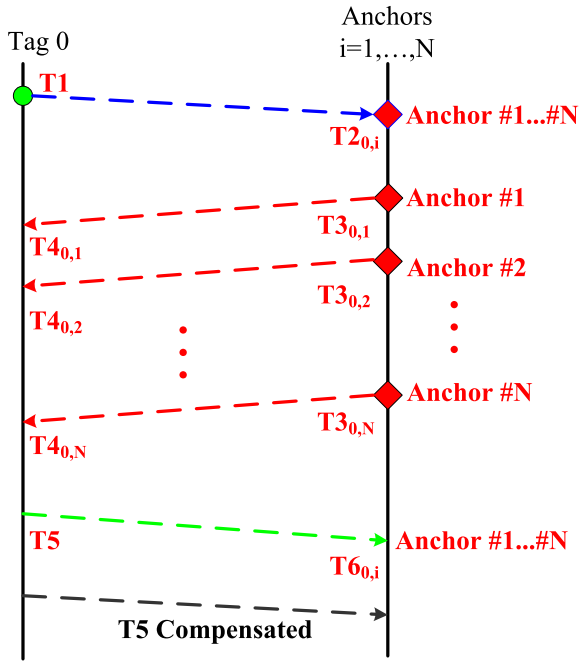

FIGURE 5. The processing of the proposed localization algorithm and timestamps measurement.

Step 2: As shown in Fig. 4(b), as the anchor's MAC address gradually grows, each anchor sends ACK messages and measures the TOE $(T3_{0,1}, T3_{0,2}, T3_{0,3}, T3_{0,4})$. The tag receives the signal and measures the TOA $(T4_{0,1}, T4_{0,2}, T4_{0,3}, T4_{0,4})$.

Step 3: As shown in Fig. 4(c), the tag broadcasts the POLL2 message and measures the TOE $(T5_0)$. All anchors receive broadcasting the signal and measure the TOA $(T6_{0,1}, T6_{0,2}, T6_{0,3}, T6_{0,4})$ via their own clocks.

Step 4: As shown in Fig. 4(d), the tag broadcasts the compensation packet, that contains $T5_0$, to Anchor 1.

At the end of the process, anchors deliver all the measured TOEs and TOAs to the localization server via Ethernet, where localization algorithms and error compensation operations are implemented. We set the time window for the tag to receive reply signals every 5 ms. This is because if the timing is too long, the energy consumption will increase.

Suppose a WSN has N anchors with known, fixed positions and a tag with an unknown position. Because the position of the tags are determined by the anchors independently, only one tag is researched in this paper (without loss of generality). First, we define $\mathbf{x}_i$ and $\mathbf{x}_0$ as the position of the anchors and tag, respectively. The $i = 1, \ldots, N$ represents the N anchors and the vectors $\mathbf{x}_i$ are all 2D or 3D. In the rest of the paper, the subscripts i refer to ith anchor and the subscripts 0 refer to the tag. Suppose all sensor nodes broadcast signals and obtain timestamps depending on their own local clocks with unknown clock skews.

III. ERROR COMPENSATED MULTI-ANCHORS TOF LOCALIZATION SCHEME

A. ESTIMATION OF CLOCK SKEW USING SDS-TWR

From (13), to reduce the estimation error for SDS-TWR, the ΔT_r, defined in (11), must be sufficiently small. This suggests that there is a limitation for the two devices' reply time that $(\bar{T}3 - \bar{T}2)$ and $(\bar{T}5 - \bar{T}4)$ should be close. Although the processing of localization algorithm in this work resembles SDS-TWR method, the proposed algorithm has no limitation on reply time because we reduce the localization error by compensating for the estimation of the relative clock skew. The workflow of the proposed algorithm is plotted in Fig. 5. To save more energy, the tag is in sleep mode until the localization algorithm is launched. The details of the proposed localization are shown as follows.

The tag sends the POLL signal and anchors receive it after the time of flight. The anchors reply to the ACK message in order and the tag receives the TOAs of ACK message depending on their MAC addresses. Then, the tag sends another POLL signal, which contains $T1$ and $T4$, and the anchors measure TOAs in the same way. Finally, $T5$ is sent for further processing. The subscript 0 represent tag and i represent ith anchor and all the sensor node measure timestamps via their own clock. For example, we define $T2_{0,1}$ to be the TOA measured by the $1th$ anchor when the former POLL message arrives from the tag.

Define $T1 \sim T6$ and $\tilde{T}1 \sim \tilde{T}6$ to be the measured and noise-free value of timestamps. We have

$$\begin{aligned} T1 &= \tilde{T}1 + n(1) \\ T2_{0,i} &= \tilde{T}2_{0,i} + n_i(2) \\ T3_{0,i} &= \tilde{T}3_{0,i} + n_i(3) \\ T4_{0,i} &= \tilde{T}4_{0,i} + n_i(4) \\ T5 &= \tilde{T}5 + n(5) \\ T6_{0,i} &= \tilde{T}6_{0,i} + n_i(6) \end{aligned} \tag{14}$$

where $i = 1, \ldots, N$ represents N anchors, $n(1) \sim n(6)$ is the associated measurement noise that can be modeled as additive white Gaussian noise (AWGN) with a zero mean and variance of σ^2.

In Fig. 5, we define $\bar{T}$ as the ideal interval of two transmission by tag. $\bar{T}$ can be obtained by two TOAs/TOEs at anchors/tag respectively.

$$\bar{T} = \frac{\tilde{T}5 - \tilde{T}1}{1 + e_0} = \frac{\tilde{T}6_{0,i} - \tilde{T}2_{0,i}}{1 + e_i} \tag{15}$$

where $(1 + e_0)$ and $(1 + e_i)$ denote the clock skew of tag and *ith* anchor respectively. Reshaping (15), we have

$$(\tilde{T}5-\tilde{T}1)-(\tilde{T}6_{0,i}-\tilde{T}2_{0,i})=e_0(\tilde{T}6_{0,i}-\tilde{T}2_{0,i})-e_i(\tilde{T}5-\tilde{T}1) \tag{16}$$

Since the clock skew of typical low cost crystal oscillator is smaller than 10ppm, we can make an approximation $1 \approx 1 - e_0 - e_i$. Whatever the value of $(\tilde{T}5 - \tilde{T}1) - (\tilde{T}6_{0,i} - \tilde{T}2_{0,i})$ in (16) is, we have

$$\begin{aligned}&(\tilde{T}5 - \tilde{T}1) - (\tilde{T}6_{0,i} - \tilde{T}2_{0,i})\\ &\quad\approx (1 - e_0 - e_i)[(\tilde{T}5 - \tilde{T}1) - (\tilde{T}6_{0,i} - \tilde{T}2_{0,i})]\end{aligned} \tag{17}$$

Combining (16) and (17) we have

$$\begin{aligned}&(\tilde{T}5 - \tilde{T}1) - (\tilde{T}6_{0,i} - \tilde{T}2_{0,i})\\ &\quad\approx e_0(\tilde{T}6_{0,i} - \tilde{T}2_{0,i}) - e_i(\tilde{T}5 - \tilde{T}1)\\ &\qquad + (e_0 + e_i)[(\tilde{T}5 - \tilde{T}1) - (\tilde{T}6_{0,i} - \tilde{T}2_{0,i})]\end{aligned} \tag{18}$$

Then

$$(\tilde{T}5-\tilde{T}1)-(\tilde{T}6_{0,i}-\tilde{T}2_{0,i}) \approx e_0(\tilde{T}5-\tilde{T}1)-e_i(\tilde{T}6_{0,i}-\tilde{T}2_{0,i}) \tag{19}$$

Combining (16) and (19) we have

$$\begin{aligned}&2[(\tilde{T}5 - \tilde{T}1) - (\tilde{T}6_{0,i} - \tilde{T}2_{0,i})]\\ &\quad\approx e_{0,i}[(\tilde{T}5 - \tilde{T}1) + (\tilde{T}6_{0,i} - \tilde{T}2_{0,i})]\end{aligned} \tag{20}$$

where $e_{0,i} = e_0 - e_i$ is the relative clock skew between the tag and the *ith* anchor. Substituting (14) into (20), (20) becomes

$$\begin{aligned}&2[(T5 - T1) - (T6_{0,i} - T2_{0,i})]\\ &\quad= e_{0,i}[(T5 - T1) + (T6_{0,i} - T2_{0,i})]\\ &\qquad + 2[n(5) - n(1) - n_i(6) + n_i(2)]\\ &\qquad - e_{0,i}[n(5) - n(1) + n_i(6) - n_i(2)]\end{aligned} \tag{21}$$

Since the clock skew is within 10ppm, the cumulative noise $[n(5) - n(1) + n_i(6) - n_i(2)] < 4 \times 10^{-9}$, the product term of noise and the clock skew in (21) is smaller than 10^{-13}, it can be ignored. So we have

$$\begin{aligned}&2[(T5 - T1) - (T6_{0,i} - T2_{0,i})]\\ &\quad\approx e_{0,i}[(T5 - T1) + (T6_{0,i} - T2_{0,i})]\\ &\qquad + 2[n(5) - n(1) - n_i(6) + n_i(2)]\end{aligned} \tag{22}$$

Stacking the N equations into matrix form

$$\mathbf{y} \approx \mathbf{Be} + \mathbf{D} \tag{23}$$

where

$$\mathbf{y} = [y_1, \ldots, y_i, \ldots, y_N]^T \tag{24}$$
$$y_i = 2[(T5 - T1) - (T6_{0,i} - T2_{0,i})] \tag{25}$$
$$\mathbf{B} = diag(b_1, \ldots, b_i, \ldots, b_N) \tag{26}$$
$$b_i = (T5 - T1) + (T6_{0,i} - T2_{0,i}) \tag{27}$$
$$\mathbf{e} = [e_{0,1}, \ldots, e_{0,i}, \ldots, e_{0,N}]^T \tag{28}$$
$$\mathbf{D} = 2[n(5) - n(1)] \cdot \mathbf{1}_N - \mathbf{D}_0\mathbf{v}_0 \tag{29}$$
$$\mathbf{D}_0 = 2\mathbf{I}_N \otimes [1, -1] \tag{30}$$
$$\mathbf{v}_0 = [n_1(6), n_1(2), \ldots, n_N(6), n_N(2)]^T \tag{31}$$

Because $\mathbf{B} = \mathbf{B}^T$, the estimation of $\mathbf{e}$ is [31]

$$\hat{\mathbf{e}} = \mathbf{B}^{-1}\mathbf{y} \tag{32}$$

Since the terms of noise in (29) and (31) are independent, the covariance matrix of $\mathbf{D}$ is

$$\begin{aligned}\mathbf{Q_D} &= E(\mathbf{D}\mathbf{D}^T)\\ &= \mathbf{D}_0\mathbf{Q}_{\mathbf{v}_0}\mathbf{D}_0^T + 8\sigma^2\mathbf{1}_N\mathbf{1}_N^T\end{aligned} \tag{33}$$

The Fisher matrix is [31]

$$J(\mathbf{e}) = \mathbf{B}^T\mathbf{Q_D}\mathbf{B} \tag{34}$$

For LSE estimation, the CRLB of the relative clock skew estimation is

$$\bar{\sigma}_e^2 = \frac{1}{N}\sum_{n=1}^{N}\left[J^{-1}\right]_{nn} \tag{35}$$

B. ERROR COMPENSATED FOR MEASURED TOF

Without loss of generality, the original biased TOF between tag and *ith* anchor can be presented by the measurement value $(T4_{0,i} - T1)$ and $(T3_{0,i} - T2_{0,i})$. We have

$$t_{p,i} = (T4_{0,i} - T1 - T3_{0,i} + T2_{0,i})/2 \tag{36}$$

Substituting (14) into (36), we have

$$\begin{aligned}t_{p,i} = &(\tilde{T}4_{0,i} - \tilde{T}1 - \tilde{T}3_{0,i} + \tilde{T}2_{0,i})/2\\ &+ [n_i(4) - n(1) - n_i(3) + n_i(2)]/2\end{aligned} \tag{37}$$

where $n(1) \sim n(4)$ refer to measurement noise. Let $\tilde{t}_{p,i}$ denotes the noise-free value of TOF, we have

$$\begin{aligned}\tilde{t}_{p,i} &= (\tilde{T}4_{0,i} - \tilde{T}1 - \tilde{T}3_{0,i} + \tilde{T}2_{0,i})/2\\ &= [(\bar{T}4_{0,i} - \bar{T}1)(1 + e_0) - (\bar{T}3_{0,i} - \bar{T}2_{0,i})(1 + e_i)]/2\end{aligned} \tag{38}$$

where $\bar{T}1 \sim \bar{T}4$ is the ideal value of timestamps. Substituting (3) into (38), we have

$$\tilde{t}_{p,i} = \bar{t}_{p,i} + [(\bar{T}4_{0,i} - \bar{T}1)e_0 - (\bar{T}3_{0,i} - \bar{T}2_{0,i})e_i]/2 \tag{39}$$

The ideal TOF also can be expressed by the propagation delay between the tag and the *ith* anchor.

$$\bar{t}_{p,i} = \|\mathbf{x}_0 - \mathbf{x}_i\|/c \tag{40}$$

where $\mathbf{x}_0$, $\mathbf{x}_i$ is the position vector of tag and the *ith* anchor, c is the velocity of light. Reshape (39), we have

$$\tilde{t}_{p,i} = \bar{t}_{p,i} + [(\bar{T}3_{0,i} - \bar{T}2_{0,i})e_{0,i}]/2 + e_0\bar{t}_{p,i} \tag{41}$$

Based on previous assumption, $|e_0\bar{t}_{p,i}|<10^{-11}$ can be ignored, we have

$$\tilde{t}_{p,i} \approx \bar{t}_{p,i} + [(\bar{T}3_{0,i} - \bar{T}2_{0,i})e_{0,i}]/2 \tag{42}$$

If $(\bar{T}3_{0,i} - \bar{T}2_{0,i})$ is a value much smaller than 1s, the difference between $(\bar{T}3_{0,i} - \bar{T}2_{0,i})$ and $(T3_{0,i} - T2_{0,i})$ is small than 10^{-5}s, (42) can be replaced by

$$\tilde{t}_{p,i} \approx \bar{t}_{p,i} + [(T3_{0,i} - T2_{0,i})e_{0,i}]/2 \tag{43}$$

Then, considering the measurement noise, we have

$$t_{p,i} \approx \bar{t}_{p,i} + [(T3_{0,i} - T2_{0,i})e_{0,i}]/2 + [n_i(4) - n(1) - n_i(3) + n_i(2)]/2 \tag{44}$$

Next, we compensate for the measured $t_{p,i}$ by using the estimation of the relative clock skew between the tag and anchor, e.g., $\hat{e}_{0,i}$, according to (32). The calibrated TOF z_i is obtained.

$$\begin{aligned} z_i &= t_{p,i} - (T3_{0,i} - T2_{0,i})\hat{e}_{0,i}/2 \\ &= \bar{t}_{p,i} + [n_i(4) - n(1) - n_i(3) + n_i(2)]/2 \end{aligned} \tag{45}$$

Combine the N calibrated TOF into matrix form

$$\mathbf{z} = f(\mathbf{x}_0) + \mathbf{w} \tag{46}$$

where

$$\mathbf{z} = [z_1, \ldots, z_i, \ldots, z_N]^T \tag{47}$$

$$z_i = t_{p,i} - (T3_{0,i} - T2_{0,i})\hat{e}_{0,i}/2 \tag{48}$$

$$f(\mathbf{x}_0) = [d_{0,1}, \ldots, d_{0.N}]^T \tag{49}$$

$$\mathbf{w} = \mathbf{C}\mathbf{u}_0 - \frac{1}{2}n(1) \cdot \mathbf{1}_N \tag{50}$$

and

$$\mathbf{C} = \frac{1}{2}\mathbf{I}_N \otimes \mathbf{C}_0 \tag{51}$$

$$\mathbf{C}_0 = [1, -1, 1] \tag{52}$$

$$\mathbf{u}_0 = [n_1(2), n_1(3), n_1(4), \ldots, n_N(2), n_N(3), n_N(4)]^T \tag{53}$$

$$\mathbf{u}_0 \sim N(0, \sigma^2\mathbf{I}_{3N}) \tag{54}$$

Since $n(1)$ and $\mathbf{u}_0$ are independent, the covariance matrix of $\mathbf{w}$ is

$$\mathbf{Q}_w = E(\mathbf{w}\mathbf{w}^T) = \mathbf{C}\mathbf{Q}_u\mathbf{C}^T + \frac{\sigma^2}{4}\mathbf{1}_N\mathbf{1}_N^T \tag{55}$$

Reshape (46), we have

$$\mathbf{z} - f(\mathbf{x}_0) = \mathbf{w} \tag{56}$$

Then the likelihood function is

$$p(\mathbf{z}, \mathbf{x}_0) = \frac{1}{(2\pi)^{N/2}det(\mathbf{Q}_w)^{1/2}} \times exp[-\frac{1}{2}(\mathbf{z} - f(\mathbf{x}_0))^T\mathbf{Q}_w^{-1}(\mathbf{z} - f(\mathbf{x}_0))] \tag{57}$$

C. MAXIMUM LIKELIHOOD ESTIMATION FOR TAG POSITION

To estimate the tag position, we use the maximum likelihood estimation (MLE) of $\mathbf{x}_0$ from (57),

$$\hat{\mathbf{x}}_0 = arg\min_{\mathbf{x}_0}(\mathbf{z} - f(\mathbf{x}_0))^T\mathbf{Q}_w^{-1}(\mathbf{z} - f(\mathbf{x}_0)) \tag{58}$$

The MLE has a least-squares interpretation because of the Gaussian measurement noise assumption. The weighted matrix is $\mathbf{Q}_w^{-1}$ and it minimizes the weighted sum of squares errors. When the function $f(\mathbf{x}_0)$ is nonlinear, the closed-form solution of (58) is not obtained. So numerical minimization is necessary, and a successive linearization procedure [22], [32] is summarized as follows:

1) $\hat{\mathbf{x}}_0(k)$ denotes the kth estimation of $\mathbf{x}_0$, and we have $\mathbf{x}_0 = \hat{\mathbf{x}}_0(k) + \Delta(k)$. Linearizing $f(\mathbf{x}_0)$ around $\hat{\mathbf{x}}_0(k)$ yields.

$$f(\mathbf{x}_0) \approx f(\hat{\mathbf{x}}_0(k)) + \mathbf{G}(\hat{\mathbf{x}}_0(k))\Delta(k) \tag{59}$$

where $\mathbf{G}(\hat{\mathbf{x}}_0(k))$ is the Jacbian matrix.

$$\mathbf{G}(\mathbf{x}_0) = \frac{\partial f(\mathbf{x}_0)}{\partial \mathbf{x}_0} \tag{60}$$

Substituting (59) to (58) and solving the linearized minimization problem for $\Delta(k)$

$$\hat{\Delta}(k) = [\mathbf{G}^T(\hat{\mathbf{x}}_0(k))\mathbf{Q}_w^{-1}(\hat{\mathbf{x}}_0(k))]^{-1} \cdot \mathbf{G}^T(\hat{\mathbf{x}}_0(k))\mathbf{Q}_w^{-1}(\hat{\mathbf{x}}_0(k)) \tag{61}$$

where

$$\mathbf{G}(\mathbf{x}_0) = \frac{1}{c}[\mathbf{r}_{1,0}^T(\mathbf{x}_0), \mathbf{r}_{2,0}^T(\mathbf{x}_0), \ldots, \mathbf{r}_{N,0}^T(\mathbf{x}_0)]^T \tag{62}$$

and $\mathbf{r}_{i,0}(\mathbf{x}_0)$ defines the unit vector.

$$\mathbf{r}_{i,0}^T(\mathbf{x}_0) = \frac{\mathbf{x}_0 - \mathbf{x}_i}{\|\mathbf{x}_0 - \mathbf{x}_i\|}, \quad i = 1, .., N. \tag{63}$$

2) The estimation at the $(k+1)th$ iteration is

$$\hat{\mathbf{x}}_0(k+1) = \hat{\mathbf{x}}_0(k) + \Delta(k) \tag{64}$$

Now, the details of the tag localization algorithm are summarized as follows:

1) The localization server collects all the timestamps $T1 \sim T6$ of the tag and anchors via Ethernet and calculates the original N TOFs using (36).
2) Compensate TOFs using (45), and the relative clock skew estimation is obtained by (32).
3) Calculate the covariance matrix $\mathbf{Q}_w$, set $k = 1$, and set the initial value of $\hat{\mathbf{x}}_0(1)$ by assigning a tag position randomly.
4) Calculate $f(\hat{\mathbf{x}}_0(k))$ and $\hat{\Delta}(k)$ using (49) and (60), respectively.
5) Update the tag position with (63); if the position change is larger than 0.1 mm, set $k = k + 1$ and go to Step 4) to continue iteration. Otherwise, the iteration stops and an estimate of the tag position is reached.

D. CRLB FOR TAG LOCALIZATION

The performance of the proposed localization algorithm is evaluated using the CRLB. The CRLB is the inverse of the Fisher information matrix. Under the Gaussian noise measurement assumption [31], [32], the Fisher matrix is

$$J(\mathbf{x}_0) = \left(\frac{\partial f(\mathbf{x}_0)}{\partial \mathbf{x}_0}\right)^T \mathbf{Q}_w^{-1} \left(\frac{\partial f(\mathbf{x}_0)}{\partial \mathbf{x}_0}\right) = \mathbf{G}^T(\mathbf{x}_0)\mathbf{Q}_w^{-1}\mathbf{G}(\mathbf{x}_0) \quad (65)$$

If the matrix $J^{-1}(\mathbf{x}_0)$ exists and the *nth* diagonal element of $J^{-1}(\mathbf{x}_0)$ is denoted by $\left[J^{-1}(\mathbf{x}_0)\right]_{nn}$, where $n = 1, 2, 3$, and the variance of any element $x_{0,n}$ of $\mathbf{x}_0$ is limited below by $\left[J^{-1}(\mathbf{x}_0)\right]_{nn}$. The CRLB of the localization estimation is

$$\tilde{\sigma}_x^2 = \sum_{n=1}^{3} \left[J^{-1}(\mathbf{x}_0)\right]_{nn}. \quad (66)$$

E. ROBUSTNESS TO MOBILITY

In this subsection, we study the influence of tag mobility for localization performance. When the tag is moving, the distances between tag-anchor pairs are changing and the tag transmits/receives at the difference positions. However, the time-of-emission (TOE) and time-of-arrival (TOA) are measured with noise. If the ranging error caused by tag mobility is smaller than the error caused by measurement noise, the proposed algorithm is robust to the tag mobility to some extent. Now, we give the restriction about robustness of the algorithm to the tag mobility as follow:

$$\frac{Pv_{tag}}{c} < \sigma_n \quad (67)$$

where P is the period of ranging operations for all tag-anchor pairs and this parameter is also called time-window of ranging. v_{tag} is the velocity of tag. c is the light speed. σ_n is the timestamp (TOE and TOA) measurement standard deviation. According to the UWB signal standard, the timestamp measurement noise σ_n is in the range of $[0.2ns, 0.5ns]$. We assume that the tag is carried by human, so $v_{tag} \leq 10m/s$. In this paper, we set the period of ranging processing P within $5ms$, while the TOE and TOA errors caused by the tag mobility in time are $\frac{Pv_{tag}}{c} < 0.17ns$. It indicates that the position changes of tag are coved or concealed by noise. Based on the above discussion, if the (67) is satisfied, the proposed algorithm presents robustness to tag mobility to some extent.

IV. NUMERICAL RESULTS

In this section, a simulation is conducted to verify the performance of the proposed method. The estimations of relative clock skew and tag location are used as input parameters. In this paper, the simulation environment resembles [22], and a two-dimensional scene is considered. Four anchors are uniformly distributed in a $100m \times 100m$ space, and are placed at $(0, 0)m$, $(0, 100)m$, $(100, 0)m$, and $(100, 100)m$. The localization server collects all the measured timestamps from the anchors and tags to estimate the relative clock skew and tag location.

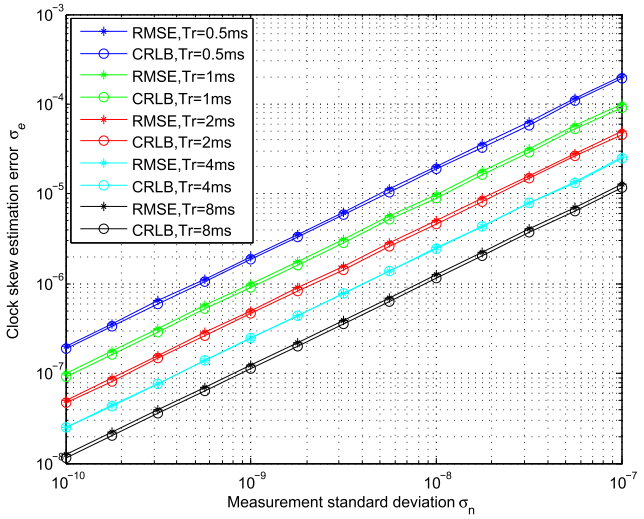

FIGURE 6. RCRLB and RMSE for relative clock skew estimation versus timestamp measurement noise for different reply time (without clock drift).

According to the clock, drift and mobility may or may not be considered. The simulations are divided into three categories. First, Monte Carlo simulations are carried out to evaluate the statistical performance of the proposed method without considering clock drift. The results consider theoretical features of the proposed algorithm. Second, a simulation with a clock drift is carried out and the performance of the estimation is analyzed. Third, the performance of mobile tag localization is studied.

A. SIMULATION FOR STATIC TAG (WITHOUT CLOCK DRIFT)

Without considering clock drift, the performance of the estimation of the relative clock skew versus the different reply times T_r (from $0.5ms$ to $8ms$) is plotted in Fig. 6. For a certain value of T_r, the root mean square error (RMSE) is close to the root CRLB (RCRLB) of the relative clock skew. We can see that the RMSE and the RCRLB of the relative clock skew are inversely proportional to the reply time. This is because the estimation of the relative clock skew is derived from (20) and is approximately weighted average of $2T_r$.

The performance of the tag localization for the proposed method is shown in Fig. 7. For comparison, the performance of the TWR method and SDS-TWR method are presented. As we can see, since the TWR method suffers from the impact of clock skew and reply time, it has a lower performance than the SDS-TWR method and our proposed method. When the standard deviation of the measurement is less than 10^{-8}, the localization error of the TWR method is kept at about 3 m (see Fig. 7). This is because the error is mainly caused by ξ_{TWR} in (6), where the $T_r = 2ms$.

Although the SDS-TWR method raises the performance of tag localization by reducing the reply time, it obviously has an extra message; thus, the relative clock skew factor also influences the localization accuracy. From Fig. 7, we clearly see that the proposed method outperforms the two methods

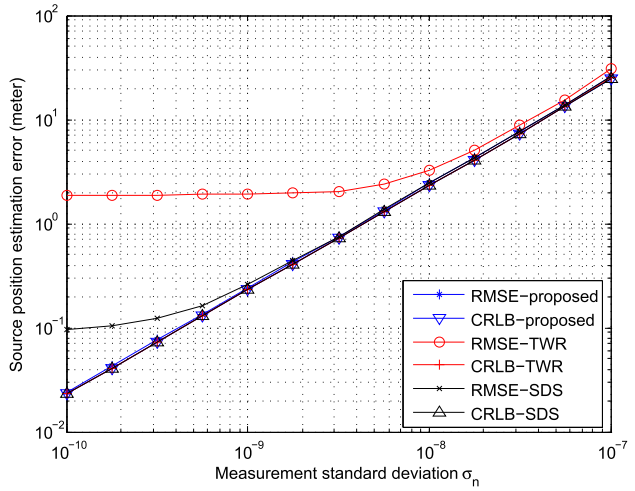

FIGURE 7. RCRLB and RMSE for tag localization estimation versus timestamp measurement noise for different methods (without clock drift). The simulation condition of TWR and SDS-TWR is same to the proposed algorithm, and $T_r = 2ms$.

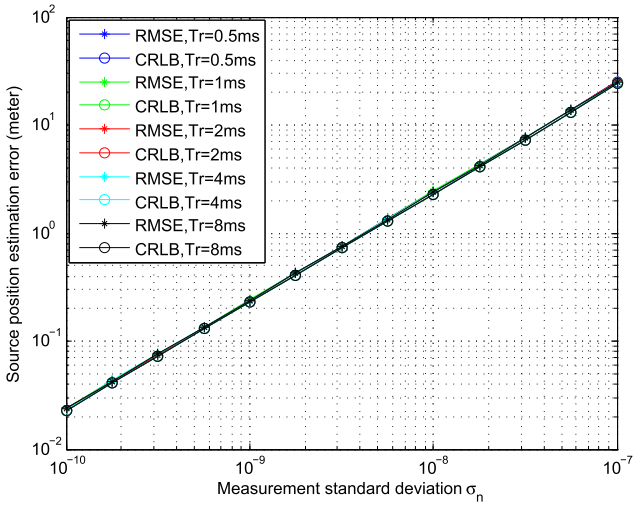

FIGURE 8. RCRLB and RMSE for tag localization estimation versus timestamp measurement noise for different methods (without clock drift).

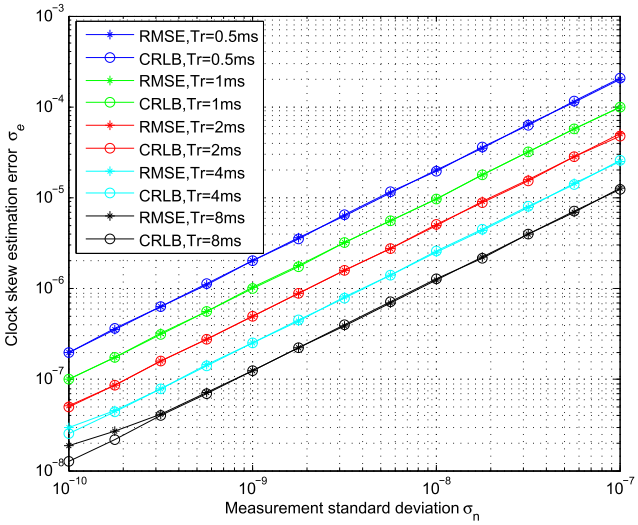

FIGURE 9. RCRLB and RMSE for relative clock skew estimation versus timestamp measurement noise for different reply time (with clock drift), where the $\sigma_f = 10^{-8}$.

when the measurement standard deviation is small; this indicates that adding the a compensation factor of the relative clock skew to the ranging scheme improves the performance. The deviation of two reply time influences the performance of the SDS-TWR algorithm, which implies a smaller reply time deviation leads to higher localization accuracy. Thus, the proposed algorithm can achieve good performance without a limitation for the reply time.

The RMSE and RCRLB of the tag localization estimate, via different reply times, are plotted in Fig. 8. The RMSE results were averaged over 10000 independent noise measurements. The figures suggests that the reply time has no effect on the tag localization performance. In the previous discussion, we concluded that the relationship between relative the clock skew and the reply time is inversely proportional. From (43), the compensated term $(T3 - T2)\hat{e}_{0,i}/2$ is proportional to the reply time. Thus, the standard deviation of calibrated TOF estimation remains constant regardless of the reply time. However, the conclusions were achieved under the assumption that the anchors and tag clock drifts are not considered. In the next section, clock drift are carried out to evaluate the performance curves of the relative clock skew and tag localization estimation.

B. SIMULATION FOR STATIC TAG (WITH CLOCK DRIFT)

In fact, the clock drift is inevitable for all kinds of clock sources; it must be considered for practical operations. In this paper, the clock frequency model resembles [33] after adding a fluctuating quartz oscillator.

$$\dot{e}_i = e_i + n_f \tag{68}$$

where n_f is AWGN with a zeros mean and variance of σ_f^2, which is depend on the practical environment (e.g., ambient temperature and working voltage).

To consider clock drift, the root mean square error (RMSE) and root CRLB (RCRLB) versus different reply times are plotted in Fig. 9. There is no obvious gap between the RMSE and corresponding RCRLB in Fig. 9. Only when the reply time $T_r = 8ms$ and the measurement standard deviation is less than 10^{-9}, does the clock drift have impact on performance. In general, clock drift has no obvious influence for the proposed localization algorithm.

The result curves for tag localization estimation, by adding clock drifts, are shown in Fig. 10. We set the $\sigma_f = 10^{-8}$ in (68). From Fig. 10, we notice that the RMSE curves of our proposed algorithm has no deviation from the RCRLB curves regardless of the measurement noise standard deviation.

The performance of the synchronous TDOA localization algorithm in [11], which is plotted with magenta curves,

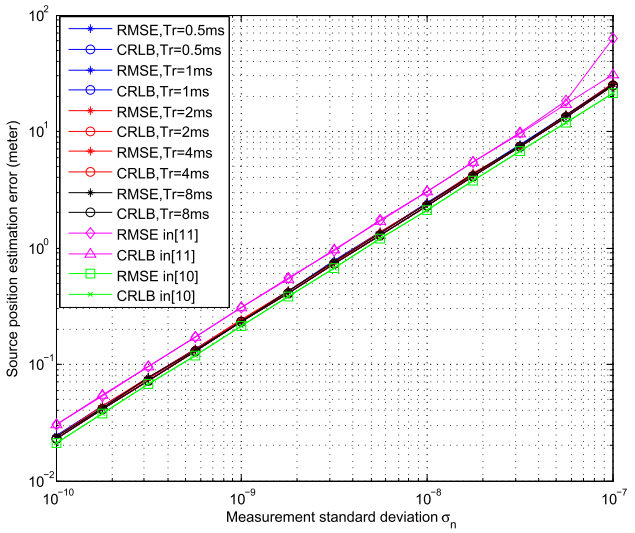

FIGURE 10. RCRLB and RMSE for tag localization estimation versus timestamp measurement noise for different methods (with clock drift), where the $\sigma_f = 10^{-8}$.

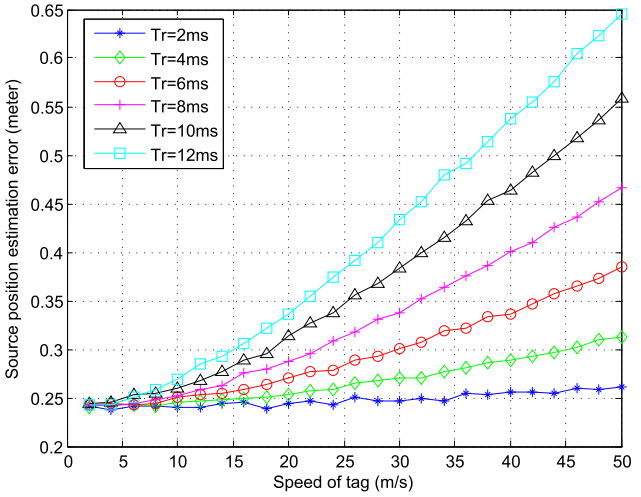

FIGURE 11. RMSE for mobile tag localization estimation versus the speed of tag for different reply time (T_r denote the reply time).

is also provided for comparison purposes in Fig. 10. Thus, the positions of the anchors are known and the anchors are well synchronized in [11]. The accuracy of algorithm in [11] is worse than those find in this paper, but the performance difference is within 3 dB. The reason is that the localization algorithm in this paper is implemented based on the TWR method and both the TOE and TOA are considered.

Furthermore, the algorithm in this paper is compared to the algorithms in [10], where a joint synchronization and localization algorithm was proposed. The RCRLB curve of this algorithm is plotted with green curves in Fig. 10. The algorithm proposed in [10] performs better than our algorithm due to a two-way message exchange method and the averaging of noisy TOAs of multiple signals from the same tag. It also can be seen that the difference between the two algorithms in localization precision, is slight and acceptable, which has little effect (in practice) on the typical values used in [34]. However, there are some preconditions for the algorithm in [10], including known timing information and localization of the anchors. The positions of the anchors is visual and measurable, but the accurate clock parameters of the anchors are difficult to obtain because of the low-quartz oscillator. Moreover, the quartz clock skew is impacted by many factors, such as working temperature, working voltage and initial working condition. Compared with the algorithm in [10] and [11], our proposed algorithm estimate the clock skew and tag localization without an accurate clock parameter in advance. Despite this limitation, our algorithm's performance is acceptable for many applications in use now.

C. SIMULATION FOR MOBILE TAG (WITHOUT CLOCK DRIFT)

Mobility is one of the most important evaluations to test the performance of a localization algorithm. A robust localization algorithm has good performance in terms of the static and mobile scene. In this subsection, we assess the performance of the proposed localization algorithm for mobile tags. Thus, the clock drift is not considered because it has little impact on our algorithm (based on previous simulation and analysis).

In this simulation, the tag performs a uniform circle motion, with a radius of 25 m and a center of (50 m, 50 m). The interval of the two consecutive localization operations is 30 ms. For each localization condition and method, we run Monte Carlo simulations with 5000 timestamp measurements. First, we present the performance of proposed algorithm versus the different reply times for various tag speeds. Second, we compare the performance of our algorithm with the TWR method and SDS-TWR methods, also for various tag speed.

From Fig. 11, we notice that the bigger reply time T_r leads to a steeper curve, which introduces a location estimation error. Obviously, if the speed of the tag is low, the performance curves (with different T_r) are close to each other. The reason is that the timestamps in (14) are measured at different times, or when tag is moving, which leads to a position-based deviation. If the tag speed is large, the position-based deviation will become more evident as time goes by. To achieve a high localization accuracy, we must reduce the reply time and localization period.

We compare the performance of our algorithm with the TWR and SDS-TWR methods at different speed values. The results are shown in Fig. 12. The proposed algorithm performs better than the TWR and SDS-TWR methods. The localization errors of the TWR and SDS-TWR methods rise rapidly as the tags move faster. In contrast, the localization error of the proposed localization algorithm appears to be insensitive to tag speed. This is because in our algorithm, a tag sends a signal to multiple anchors and all the anchors receive the signal. After a sufficient reply time, the anchors send the reply message depending on MAC address (from small to large). However, the TWR and SDS-TWR methods only

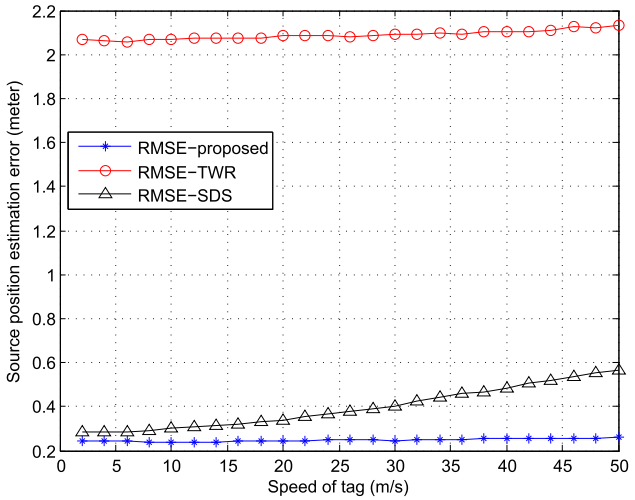

FIGURE 12. RMSE for mobile tag localization estimation versus the speed of tag for different methods ($T_r = 2ms$ denote the reply time).

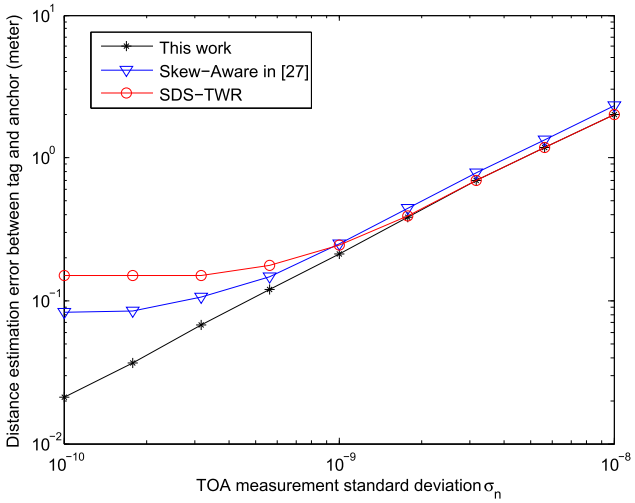

FIGURE 13. Comparison of ranging measurement between the proposed algorithm and existing algorithms.

measure the range between a tag and one of the anchors at a time. If there are N anchors, one complete localization period is $N(2t_p + T_r)$ for TWR, $N(3t_p + 2T_r)$ for SDS-TWR and $(3t_p + 2T_r)$ for our proposed algorithm. We can also conclude that the localization error of the SDS-TWR rises faster than that of the TWR as the value of the tag speed is growing. This is shown in Fig. 12.

D. COMPARISON WITH OTHER METHODS

The comparison of our proposed method with the Skew-Aware [27] and SDS-TWR methods, in term of ranging measurement, are shown in Fig. 13. The Skew-Aware method is developed from the TWR algorithm. A linear regression approach is adopted to compensate for the clock skew in this method. In this simulation, we set the number of successive historical messages to 32 for the Skew-Aware method.

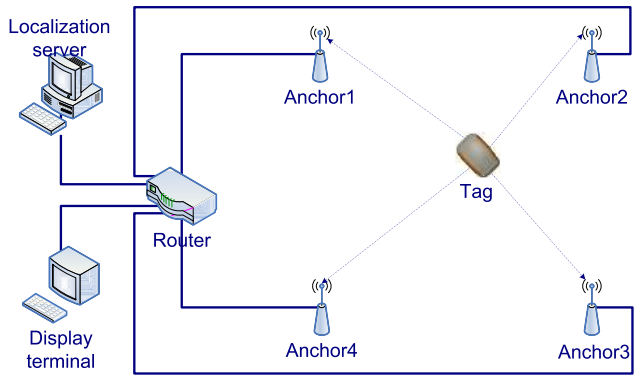

FIGURE 14. System structure.

From the simulation results in Fig. 13, the performance of the Skew-Aware method is better than the SDS-TWR method when the TOA measurement standard deviation is less than 10^{-9}. This is because there is a clock skew estimation based on historical TOF measurements in the Skew-Aware method. This suggests that a small noise level leads to accurate clock skew estimation. Thus, the ranging error caused by clock skew can be compensated for in the Skew-Aware method. However, as the noise level increases, the accuracy of the clock skew in the Skew-Aware method is limited by the noisy TOF measurements.

As shown in Fig. 13, the performance of our proposed method is better than that of the Skew-Aware method. Although both our proposed method and the Skew-Aware method reduce the effects of clock skew via estimation and compensation operations, the proposed method obtains a relative clock skew estimation based on the SDS-TWR timing stamps while the Skew-Aware method is based on the TWR method. In fact, longer time span for clock skew can result in more accurate skew estimation, especially in noisy environment. On the other hand, the Skew-Aware method is implemented using a series of historical messages that are transmitting measurements continuously while only the current timing stamps are considered for our proposed method. Thus, our proposed method is simple, efficient and effective.

V. EXPERIMENTS

This section introduces the architecture of the localization system employed in this study. We illustrate the hardware for the anchor and tag. Then, the experiment performance is demonstrated and compared with the traditional SDS-TWR algorithm.

A. EXPERIMENT SYSTEM

1) SYSTEM STRUCTURE

To implement our experiment, a specific experimental framework is needed. This framework is shown in Fig. 14. The system is comprised of four components (e.g., anchors, a tag, a localization server and a display terminal). The wireless signal model is ultra-wideband (UWB) radio compliant that

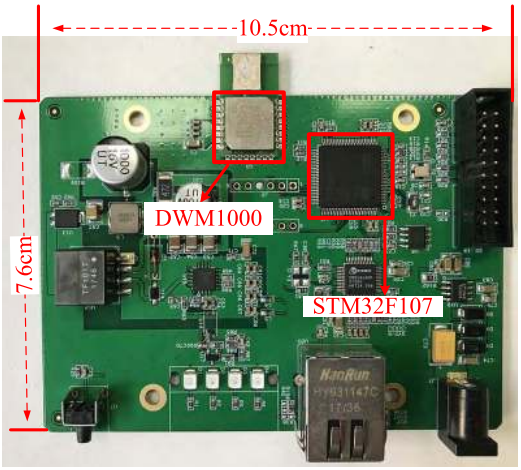

FIGURE 15. Anchor hardware.

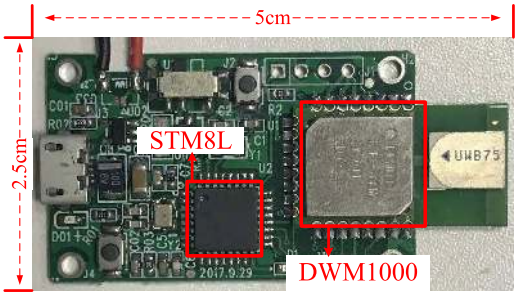

FIGURE 16. Tag hardware.

satisfies IEEE 802.15.4a-2011. The working frequency range is from 3.5 to 6.5 GHz.

We use a DW1000 radio transceiver in the anchor and the tag. The DW1000 module is based on the DW1000 chip developed by DecaWave company and is compatible with the IEEE 802.15.4-2011 protocol for UWB radio transceiver chips. The DWM1000 has strange anti-interference ability for multi-path fading and reliable communication in complex electromagnetic environment. The maximum rate of data transmission can reach 6.8 Mb/s.

2) ANCHOR

The hardware diagram of the anchor is shown in Fig. 15. The radio transceiver module is DecaWave DW1000, which abides by the IEEE802.15.4a standard. The controlling module is the STM32F107VCT6 chip. Anchors are powered over Ethernet (POE) technology that abides by the IEEE 802.3af standard.

3) TAG NODE

The hardware diagram of the tag is shown in Fig. 16. Although tags have low power consumption requirement, small size and high stability, the DWM1000 can be applied to the tags. The controlling module for the tags is the STM8L151 chip.

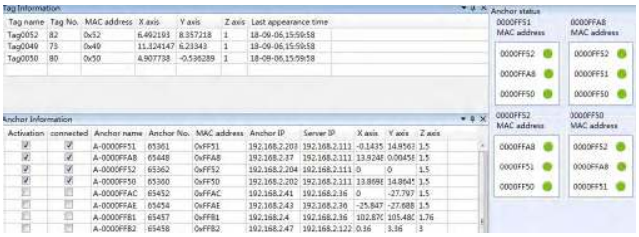

FIGURE 17. Localization server.

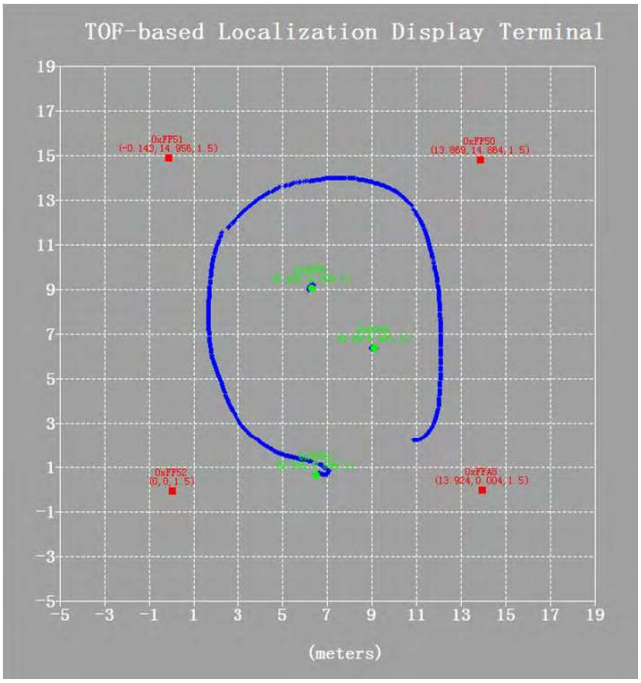

FIGURE 18. Display terminal (red point present anchor; blue point present the historical location of tag; green point present the current location of tag).

4) LOCALIZATION SERVER

A localization server that runs on a personal computer (PC). The relative clock skews between tag-anchor pairs are estimated and the position of tag is determined in the localization server. The localization server also configures the anchor parameters and monitors the condition. An example of the running interface for the localization server is shown in Fig. 17.

5) DISPLAY TERMINAL

The display terminal can dynamically show the historical position and current position of the tag. An example of the display terminal interface is shown in Fig. 18. From Fig. 18, we can see two static tags and a mobile tag. The blue cross '+', which was plotted using the historical tag positions, can be used to find the present tag's moving track. The green solid circles represent the current tag's position. The red solid rectangles represent the anchor's positions.

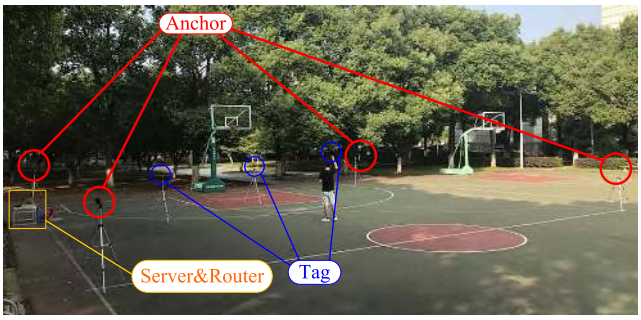

FIGURE 19. Experiment environment.

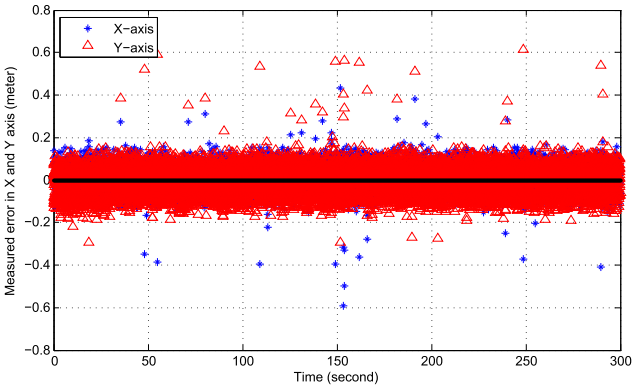

FIGURE 20. Coordinate error contain X and Y axis versus time.

B. EXPERIMENT SCENE

To evaluate the performance of the proposed localization algorithm, we performed extensive experiments via an actual asynchronous WSN. Fig. 19 shows the experiment scene. For convenience, a 2D localization scene in a basketball court is considered. The experiment system consists of four anchors, a tag, a router, and a PC. We implemented the experiment in a $15 \times 14\ m^2$ space. The four anchors were placed at $(0, 0)$, $(15\ m, 0)$, $(15\ m, 14\ m)$ and $(0, 14\ m)$. The position of the tag is $(7.3m, 8.6m)$. The tag and anchor measure the TOE and TOA independently. A single localization period is 30 ms and the opening window of the tag is 5 ms.

C. EXPERIMENT RESULT

To locate a tag, we need at least three ranging measurements based on the TOF localization algorithm. Tag and anchors measured the TOEs and TOAs on their own clock, respectively. The measured timestamps were used for estimating the relative clock skew and computing the original TOFs. Then, the localization server compensated for the original TOF via relative clock skew estimations and by estimating the tag location via the MLE method.

We implemented the experiment for 300 seconds. Because the single localization period is 30 ms, we can obtain approximately 10000 coordinate positions. The coordinate errors consist of changes in X and Y over the experiment period.

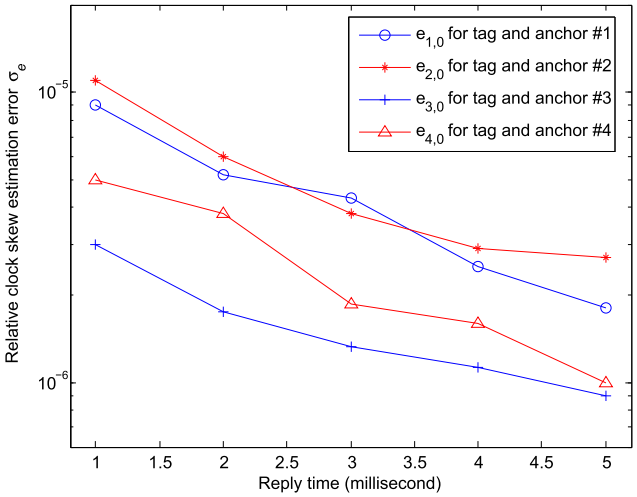

FIGURE 21. Relative clock skew estimation versus reply time (The horizontal coordinate-axis X is presented by linear scale, the longitudinal coordinate-axis Y is presented by logarithmic scale).

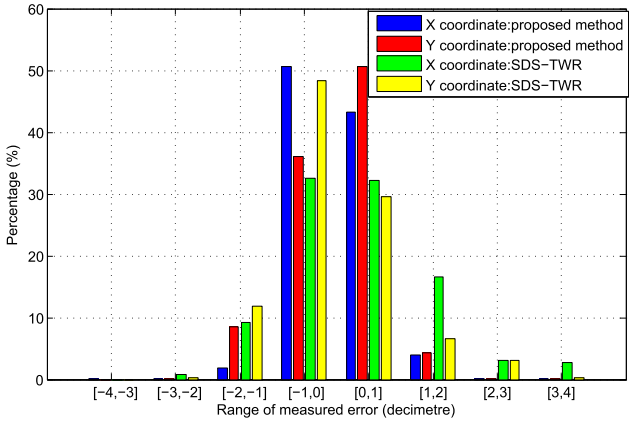

FIGURE 22. Distribution of coordinate error.

This information is plotted in Fig. 20. Thus, most of the results for the coordinate error were less than 0.2 m.

Fig. 21 shows the performance of the relative clock estimation versus reply time. We implement the estimation of the relative clock skew for 5000 times, each with a fixed reply time. The true values of the clock skews in practice are difficult to obtain because there are many random factors that have an influence on them. For this reason, the errors of relative clock skew estimations are denoted by a sample standard deviation, where the $e_{i,0}, i = 1 \ldots 4$ in Fig. 21 denotes the relative clock skew between the tag and the *ith* anchor. In Fig. 21, the error of the relative clock skew estimation decreases as the reply time increases. In fact, the relative clock skew is estimated using (20). Since the TOF between the tag and the anchor is much smaller than the reply time, the denominator of (20) is mainly decided by the reply time. This indicates that the error of the relative clock skew estimate is approximately weighted average of double reply time ($2T_r$), which has the same implication as Fig. 6.

TABLE 2. Compare with existing algorithm.

Method	System	Mean	RMSE	Complexity	$\Delta T_r \approx 0$
SDS-TWR	Our	0.127m	0.159m	Medium	Yes
Proposed	Our	0.078m	0.089m	Low	No

$\Delta T_r \approx 0$ presents the requirement for the value of reply time ΔT_r must be small.

Fig. 22 shows the distribution of coordinate errors by comparing our results with the result of using the traditional SDS-TWR algorithm. For our proposed algorithm, the coordinate error has a precision of 86% within 0.1 m. For SDS-TWR, the coordinate error has a precision of 65% within 0.1 m. There is also a limitation for the reply time in SDS-TWR. Although we set the two reply times in (11) as small as possible when implemented in the experiment, this action is also sensitive to the speed of light. The relative clock skew e_{AB} in (45) is compensated by our proposed algorithm. Thus, our proposed algorithm is better than SDS-TWR.

The RMSE of localization error can be computed by

$$RMSE = \sqrt{\frac{\sum_{i=1}^{M} \|\mathbf{x}_i - \mathbf{x}\|^2}{M}} \tag{69}$$

where $\mathbf{x}_i$ and $\mathbf{x}$ denoted the measured position of tag and the true position of tag, M denoted the number of localization measurement.

We compared the performance of the proposed algorithm with the SDS-TWR method in the same experiment environment. The results are shown in Table. 2. The proposed algorithm can obtain higher localization accuracy without an additional restriction on the reply time.

VI. CONCLUSION

In this paper, we show that the clock skew has a significant impact on the performance of time-based localization algorithms. Because a 3 ns error in time results in a 1 m ranging error, we propose a robust compensated multi-anchors TOF localization algorithm for asynchronous wireless sensor networks to mitigate the ranging errors. To synchronize the clock parameters of the tag-anchor pairs, the relative clock skew is estimated via least squares estimation (LSM). The original TOF measurement is calibrated via the estimation of the relative clock skew. A linearized maximum likelihood estimation (MLE) is adopted for the tag localization problem. Thus, the proposed localization approach is simple, effective and particularly suited for low-quality crystal oscillator-based systems. Our simulation shows that the performance of the localization algorithm in this paper is close to the CRLB curves. The localization accuracy outperforms traditional methods using a typical low-cast crystal oscillator. Furthermore, the clock drift has little impact on the localization accuracy based on simulation result and previous discussion. Our experiment provides the actual observation results to evaluate the localization accuracy, so that the tag position can be correctly determined in our method.

REFERENCES

[1] I. F. Akyildiz, W. Su, Y. Sankarasubramaniam, and E. Cayirci, "A survey on sensor networks," *IEEE Commun. Mag.*, vol. 40, no. 8, pp. 102–114, Aug. 2002.

[2] G. Smart, N. Deligiannis, R. Surace, V. Loscri, G. Fortino, and Y. Andreopoulos, "Decentralized time-synchronized channel swapping for ad hoc wireless networks," *IEEE Trans. Veh. Technol.*, vol. 65, no. 10, pp. 8538–8553, Oct. 2016.

[3] D. N. Hatfield, "A report on technical and operational issues impacting the provision of wireless enhanced 911 services," Dept. Transp., Federal Commun. Commission, Washington, DC, USA, Tech. Rep., 2003.

[4] K. Lorincz *et al.*, "Sensor networks for emergency response: Challenges and opportunities," *IEEE Pervasive Comput.*, vol. 3, no. 4, pp. 16–23, Oct./Dec. 2004.

[5] K. Zhou and S. I. Roumeliotis, "Multirobot active target tracking with combinations of relative observations," *IEEE Trans. Robot.*, vol. 27, no. 4, pp. 678–695, Aug. 2011.

[6] H. Liu, H. Darabi, P. Banerjee, and J. Liu, "Survey of wireless indoor positioning techniques and systems," *IEEE Trans. Syst., Man, Cybern. C, Appl. Rev.*, vol. 37, no. 6, pp. 1067–1080, Nov. 2007.

[7] F. Dwiyasa and M. H. Lim, "A survey of problems and approaches in wireless-based indoor positioning," in *Proc. Int. Conf. Indoor Positioning Indoor Navigat. (IPIN)*, Oct. 2016, pp. 1–7.

[8] Y. Wang, X. Ma, and G. Leus, "Robust time-based localization for asynchronous networks," *IEEE Trans. Signal Process.*, vol. 59, no. 9, pp. 4397–4410, Sep. 2011.

[9] A. Tahat, G. Kaddoum, S. Yousefi, S. Valaee, and F. Gagnon, "A look at the recent wireless positioning techniques with a focus on algorithms for moving receivers," *IEEE Access*, vol. 4, pp. 6652–6680, 2017.

[10] J. Zheng and Y.-C. Wu, "Joint time synchronization and localization of an unknown node in wireless sensor networks," *IEEE Trans. Signal Process.*, vol. 58, no. 3, pp. 1309–1320, Mar. 2010.

[11] R. M. Vaghefi and R. M. Buehrer, "Asynchronous time-of-arrival-based source localization," in *Proc. IEEE Int. Conf. Acoust., Speech Signal Process.*, May 2013, pp. 4086–4090.

[12] Q. Luo, Y. Peng, J. Li, and X. Peng, "RSSI-based localization through uncertain data mapping for wireless sensor networks," *IEEE Sensors J.*, vol. 16, no. 9, pp. 3155–3162, May 2016.

[13] K. Lin, M. Chen, J. Deng, M. M. Hassan, and G. Fortino, "Enhanced fingerprinting and trajectory prediction for IoT localization in smart buildings," *IEEE Trans. Autom. Sci. Eng.*, vol. 13, no. 3, pp. 1294–1307, Jul. 2016.

[14] L. Liu and H. Liu, "Joint estimation of DOA and TDOA of multiple reflections in mobile communications," *IEEE Access*, vol. 4, pp. 3815–3823, 2016.

[15] N. H. Nguyen and K. Doğançay, "Optimal geometry analysis for multistatic TOA localization," *IEEE Trans. Signal Process.*, vol. 64, no. 16, pp. 4180–4193, Aug. 2016.

[16] G. Wang, A. M.-C. So, and Y. Li, "Robust convex approximation methods for TDOA-based localization under NLOS conditions," *IEEE Trans. Signal Process.*, vol. 64, no. 13, pp. 3281–3296, Jul. 2016.

[17] F. Gustafsson and F. Gunnarsson, "Mobile positioning using wireless networks: Possibilities and fundamental limitations based on available wireless network measurements," *IEEE Signal Process. Mag.*, vol. 22, no. 4, pp. 41–53, Jul. 2005.

[18] S. Gezici, "A survey on wireless position estimation," *Wireless Personal Commun.*, vol. 44, no. 3, pp. 263–282, Feb. 2008.

[19] S. Ganeriwal, R. Kumar, S. Adlakha, and M. B. Srivastava, "Network-wide time synchronization in sensor networks," NESL, Bengaluru, India, Tech. Rep., 2003.

[20] S. Jain and Y. Sharma, "Optimal performance reference broadcast synchronization (OPRBS) for time synchronization in wireless sensor networks," in *Proc. Int. Conf. Comput., Commun. Elect. Technol.*, 2011, pp. 171–175.

[21] N. Xu, X. Zhang, Q. Wang, J. Liang, G. Pan, and M. Zhang, "An improved flooding time synchronization protocol for industrial wireless networks," in *Proc. Int. Conf. Embedded Softw. Syst.*, 2009, pp. 524–529.

[22] H. Xiong, Z. Chen, W. An, and B. Yang, "Robust TDOA localization algorithm for asynchronous wireless sensor networks," *Int. J. Distrib. Sensor Netw.*, vol. 11, no. 5, p. 10, 2015.

[23] F. Zhang, G. Wang, and W. Wang, "Novel two-step method for joint synchronization and localization in asynchronous networks," *IEEE Wireless Commun. Lett.*, vol. 6, no. 6, pp. 830–833, Dec. 2017.

[24] M. R. Gholami, S. Gezici, E. G. Strom, and M. Rydstrom, "Hybrid TW-TOA/TDOA positioning algorithms for cooperative wireless networks," in *Proc. IEEE Int. Conf. Commun.*, Jun. 2011, pp. 1–5.

[25] R. Hach, *Symmetric Double Side Two-Way Ranging*, IEEE Standard P802.15 Working Group for Wireless Personal Area Networks (WPAN), Jun. 2005.
[26] R. Exel and T. Sauter, "Carrier-aided clock skew estimation for TOA ranging with minimal overhead," in *Proc. Factory Commun. Syst.*, 2014, pp. 1–8.
[27] F. Despaux, K. Jaffrès-Runser, A. van den Bossche, and T. Val, "Accurate and platform-agnostic time-of-flight estimation in ultra-wide band," in *Proc. IEEE Int. Symp. Pers., Indoor, Mobile Radio Commun.*, Sep. 2016, pp. 1–7.
[28] S. Gao, S. Zhang, G. Wang, and Y. Li, "Robust second-order cone relaxation for TW-TOA-based localization with clock imperfection," *IEEE Signal Process. Lett.*, vol. 23, no. 8, pp. 1047–1051, Aug. 2016.
[29] B. Etzlinger and H. Wymeersch, "Synchronization and localization in wireless networks," *Found. Trends Signal Process.*, vol. 12, no. 1, pp. 1–106, 2018.
[30] D. Oh, S. Go, and J. Chong, "Packet-reduced ranging method with super-resolution TOA estimation algorithm for chirp-based RTLS," *ETRI J.*, vol. 35, no. 3, pp. 361–370, 2013.
[31] S. M. Kay, *Fundamentals of Statistical Signal Processing: Estimation Theory*. Englewood Cliffs, NJ, USA: Prentice-Hall, 1993.
[32] T. Li, A. Ekpenyong, and Y. F. Huang, "Source localization and tracking using distributed asynchronous sensors," *IEEE Trans. Signal Process.*, vol. 54, no. 10, pp. 3991–4003, Oct. 2006.
[33] G. Giorgi, "An event-based Kalman filter for clock synchronization," *IEEE Trans. Instrum. Meas.*, vol. 64, no. 2, pp. 449–457, Feb. 2015.
[34] *IEEE Standard for Information Technology—Local and Metropolitan Area Networks—Specific Requirements—Part 15.4: Wireless Medium Access Control (MAC) and Physical Layer (PHY) Specifications for Low-Rate Wireless Personal Area Networks (WPANs): Amendment 1: Add Alternate PHYs*, IEEE Standard 802.15.4a-2007, 2007, pp. 1–203.

TAN WANG received the B.S. degree in electronic information science and technology from Lanzhou University, in 2013, and the M.S. degree in information and communication engineering from the National University of Defense Technology (NUDT), in 2015, where he is currently pursuing the Ph.D. degree in information and communication engineering. His research interests include wireless sensor networks, wireless communication, and information processing.

HONG DING was born in Suqian, Jiangsu, China, in 1973. She received the Ph.D. degree in electrical engineering from the National University of Defense Technology (NUDT), China, where she is currently an Associate Professor. Her research interests include signal detection and estimation, UWB ranging and localization, and wireless communication.

HUI XIONG was born in Hubei, China, in 1970. He received the M.S. and Ph.D. degrees in communication and information system from the National University of Defense Technology (NUDT), Changsha, China, in 1995 and 1998, respectively, where he is currently an Associate Professor with the School of Electronic Science and Technology. His research interests include wireless sensor network localization and communication signal processing.

LINHUA ZHENG was born in Hunan, China, in 1961. He received the M.S. degree from the Huazhong University of Science and Technology, in 1985, and the Ph.D. degree from the National University of Defense Technology, Changsha, China, in 2003, where he is currently a Full Professor with the School of Electronic Science and Technology. His research interests include satellite communication, measurement and control communication, channel coding, and wireless communication.